UDC 621.396.43

EFFICIENCY OF SPATIAL SIGNAL PROCESSING IN WIRELESS COMMUNICATIONS

Gleb L. Avdeyenko, Maxim A. Kolomytsev, Yevgeniy A. Yakornov

National Technical University of Ukraine “KPI”, Kyiv, Ukraine

The mathematical modeling of amplitude and phase distribution of the electromagnetic fields at the aperture of the receiving antenna system has been performed. The possibility of frequency reuse in radio relay link under condition when two transmitters operate simultaneously on the same frequency and with same polarization is substantially investigated by using the phenomenon of phase front curvature of electromagnetic wave. An effective approach to optimal spatial processing of two radio signals from two transmitters at the receiving side of radio relay link is developed. The mathematical expressions allowing the theoretical analysis of spatial processing of radio relay link signals are obtained. The results of theoretical investigations are extensively discussed. The references for practical application of obtained results at the development of microwave link equipment are given.

Introduction

An evolution of wireless telecommunication networks follows the way of broadening the information services and improvement of their quality. The quality of services improvement can be achieved by using additional frequency bands. Therefore, the effective use of frequency spectrum is one of the most important problems in wireless communications applying the digital radio relay systems (DRRS) designed for building telecommunication network backbones.

The spectrum scarcity problem for DRRS can be solved either by increasing channels number without modulation change or by multipositional modulation of digital signals such as QAM-16, QAM-32, QAM-64, QAM-128, QAM-256 without any change in bandwidth. The latter approach is widely used in practice and provides high spectrum efficiency as compared with QPSK modulation. On the other hand, this approach can be applied in the case of stability for both high frequency carrier and heterodyne low phase noise. Significant signal to noise ratio for radio relay receivers is also required (when QAM-64 is used, signal to noise ratio equals to 33 dB) [1]. Therefore, it is advisable to continue the researches in order to increase the effectiveness of using the spectrum allocated for DRRS with multipositional modulation by sophistication of existing signal selection methods. It is important to investigate the electromagnetic wave features as an appropriate way to provide separation of radio signals operating in the same frequency band at receiving side with minimum signal distortions. It can be supposed that one of the ways to solve these important problems consists in applying such physical effect as electromagnetic wave (EMW) phase front curvature in the process of radio frequency reuse. This physical effect has been successfully employed to resolution of different scientific tasks for modern radio and acoustic techniques, in particular for interference discrimination [2] and for the determination of radiation sources coordinates [3, 4].

Statement of the problem

The purpose of the paper is to investigate the possibility of applying such physical effect as EMW phase front curvature of radiation source to develop the approach for separation of two different radio signals at receiving side by using the frequency reuse. The frequency reuse principle implementation can provide the reliable transmission of two radio signals simultaneously radiated by two different radio sources in the same frequency band and with the same polarization. It is presumed that radiation sources are located at the same distance from receiving side point of DRRS but spaced from each other [2, 5].

The idea of the proposed approach is based on the common usage of spatial signal processing in sparse antenna array of transmitting and receiving parts of radio relay system. The formation of two independent EMW radiation sources on transmitting part takes place in the same frequency band and with the same polarization when, for example, the information traffic from different telecommunication operators is transmitted. The electromagnetic fields radiated by these sources form different EMW phase fronts at the aperture of receiving sparse antenna array. These phase fronts should have the shapes of different curvature in order to realize the considered principle. If the signal radiated by the first source generates a plane front in receiving point, the phase front formed by second source should have any other shape. If both sources form the spherical

© 2012, National Technical University of Ukraine “Kyiv Polytechnic Institute”

phase fronts, their curvatures must be different. The optimal spatial signal processing is exercised in receiving antenna array in order to separate radio signals with different forms of phase front ensuring minimal energy loss and maximal isolation from each other.

As a component of proposed approach of frequency reuse by spatial processing, the analysis of EMW amplitude and phase distributions at the continuous aperture of receiving side antenna must be performed. The purpose of this analysis is to prove the possibility of phase front curvature creation by sparse antenna array of transmitting side. When the required curvature creation is completed, spatial signal processing at receiving sparse antenna array and its effectiveness can be analyzed. The particular case of continuous aperture of receiving sparse antenna array will be considered.

To simplify the analysis at the first stage, the following restrictions are introduced. Radio waves propagation medium between transmitter and receiver is homogenous and isotropic. The form of phase front is not distorted along the propagation path. The influence of multipath propagation and fading in receiving side is absent. The shielding and reflecting obstacles are absent in first Fresnel zone. Random errors of amplitude and phase distribution at the sparse aperture array of transmitting and receiving parts are not considered. The separation distance between antenna systems of transmitting and receiving parts of DRRS satisfies conditions of receiving part location at Fresnel zone of the transmitting part:

$$D_{NF.TR} << D << D_{FF.TR}, \qquad (1)$$

where $D_{NF.TR} = 0.62\sqrt{L_{p1}^3/\lambda}$, $D_{FF.TR} = 2L_{p1}^2/\lambda$ are near-field and far-field region contours for sparse antenna array; $L_{p1} = (M-1)L_1 + D_{A.TR}$ is the length of transmitting antenna array aperture; $D_{A.TR}$ denotes the diameter of transmitting antenna; M is the number of antennas; λ is the wave length in free space.

Antenna elements of transmitting side are considered as point radiation sources because ratio of antenna diameter to separation distance between transmitting and receiving parts is less than unity.

To simplify the further analysis, we consider spatial signal processing for simplex DRRS. However, the analysis technique considered below can be applied for duplex DRRS.

EMW amplitude and phase distribution on the receiving continuous aperture

Let us define the conditions under which the EMW phase front will have required curvature at the receiving side aperture of sparse antenna array. For example, we calculate the amplitude and phase distributions of EMW at receiving side continuous aperture of cophased three-element sparse antenna array. When the phase distribution law will be non-linear, a physical effect of EMW phase front curvature or effect of its sphericity in particular case can be observed.

Let us consider the DRRS with spatial processing simplified structure schematically depicted in Fig. 1 where the point O designates the center of the aperture. According to this schema, one can determine the angles created by EMW of each three transmitting side antennas coming into random point X of receiving side aperture:

$$\theta_{0x}(x) = \arctan(x/d); \; \theta_{1x}(x) = \arctan[(L_{tr.1} - x)/d];$$
$$\theta_{2x}(x) = \arctan[(L_{tr.2} + x)/d]. \qquad (2)$$

Taking into account that the DRRS radio signal of each channel satisfies the narrow band condition $\Delta f / f_0 << 1$, where Δf is frequency band occupied by the radio signal; f_0 is its carrier frequency, the total radio signal in the point X generated by electromagnetic wave interference from different antennas of array can be presented as:

$$\dot{s}_0(t,x) = \sum_{i=0}^{2} \alpha_i \dot{s}_{tr}[t - d_{ix}(x)/c] F_{i.tr}[\theta_{ix}(x)], \qquad (3)$$

where $\omega_0 = 2\pi f_0$; $\dot{s}_{tr}(t) = \dot{S}_{tr}(t)\exp(j\omega_0 t)$ designates the complex time form of desired signal at transmitting side; $\dot{S}_{tr}(t) = S_{tr}(t)\exp[j\Psi(t)]$ denotes the complex envelope of desired signal; $S_{tr}(t)$, $\Psi(t)$ are the real envelope of desired signal and its phase, respectively; $F_{i.tr}(\theta)$ denotes the beam pattern of ith transmitting antenna in angle direction θ; $\alpha_0, \alpha_1, \alpha_2$ are dimensionless coefficients taking into account transmitting antenna gain G_{tr}, free space energy losses L_0 along propagation path between transmitter and receiver due to divergence of EMW wave front, hydrometeor absorption L_{atm}, difference of polarizations of receiving and transmitting antennas and other losses L_{add}. Free space energy losses are defined by the formula $L_0 = 20\log(4\pi d/\lambda)$, where λ is wavelength; d denotes the distance between transmitter and receiver.

Assuming that the propagation conditions for different radio beams of transmitting antennas are the same, we can consider that $\alpha_0 = \alpha_1 = \alpha_2 = 10^{0.05 L_\Sigma}$, where $L_\Sigma = L_0 + L_{att} + L_{add} - G_{tr}$, dB. These conditions allow simple determination of distances from transmitting side antennas to aperture point X that are denoted in Fig. 1 as $d_{1x}(x)$ and $d_{2x}(x)$:

$$d_{0x}(x) = \sqrt{x^2 + d^2}; \; d_{1x}(x) = \sqrt{(L_{tr.1} - x)^2 + d^2};$$

$$d_{2x}(x) = \sqrt{(L_{tr.2} + x)^2 + d^2}\ . \qquad (4)$$

To simplify further calculations, we omit the variable x in some cases.

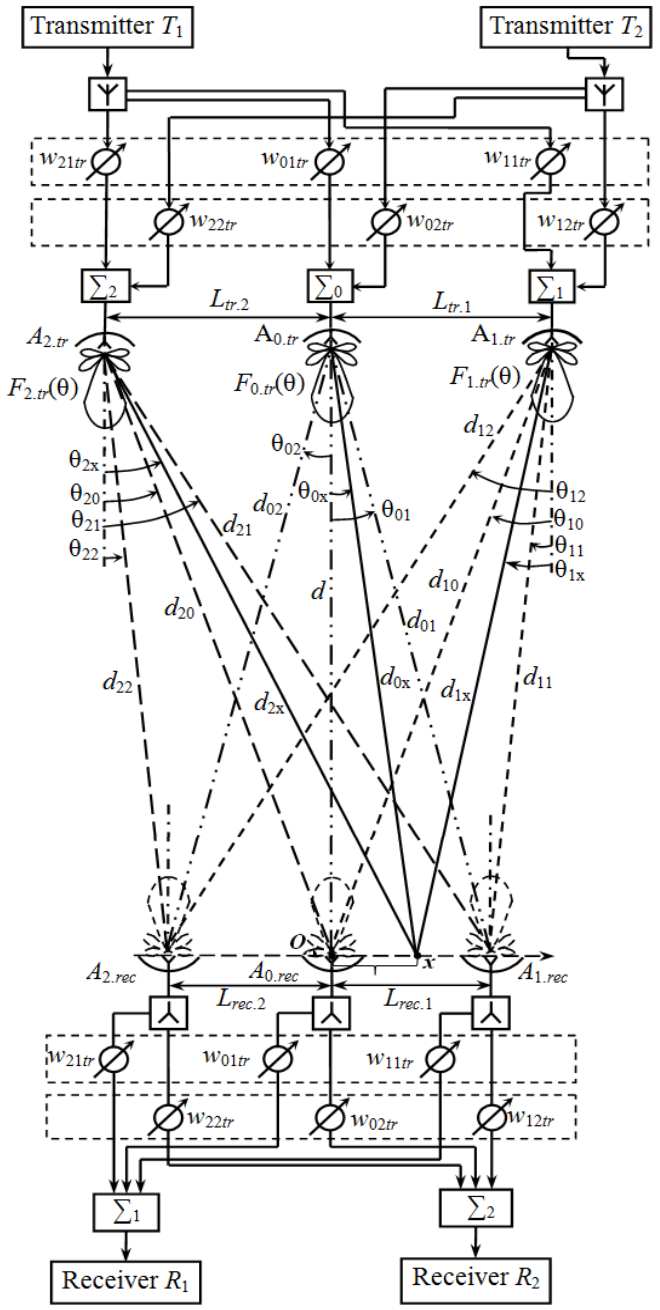

Fig. 1. Structure diagram of DRRS transmitting and receiving sides based on sparse antenna arrays.

Let us consider the simplest case of spatial processing at transmitting side when radio signal from the transmitter T_1 is radiated by all three antennas and radio signal from the transmitter T_2 is radiated only by central antenna of transmitting sparse antenna array. In this case, the following weighting coefficients of spatial processing blocks of transmitting side depicted in Fig. 1 by chain lines can be believed as $w_{01tr} = w_{11tr} = w_{21tr} = 1$; $w_{12tr} = w_{22tr} = 0$; $w_{02tr} = 1$.

The highest possible size of receiving antenna array aperture L_{rec} can be chosen using the narrowband feature conditions of space-time radio signal. According to Fig. 1, these conditions can be written as follows:

$$(d_{02} - d)/c << 1/\Delta f\ ;\ (d_{01} - d)/c << 1/\Delta f\ ; \qquad (5)$$

$$(d_{12} - d_{11})/c << 1/\Delta f\ ;\ (d_{21} - d_{22})/c << 1/\Delta f\ . \qquad (6)$$

Expressions (5) describe the conditions of space-time radio signal narrowband feature at the aperture of receiving sparse antenna array for spherical phase front of EMW radiated by antenna A_{0tr}. Taking into account relations (4), these conditions can be formulated in such a way:

$$d_{01} = \sqrt{L_{rec.1}^2 + d^2}\ ;\ d_{02} = \sqrt{L_{rec.2}^2 + d^2}\ . \qquad (7)$$

Because $L_{rec.1}/d << 1$; $L_{rec.2}/d << 1$, we can limit by second order terms of Taylor series expansions of expressions (7). As a result, we obtain

$$d_{01} \approx d + L_{\text{rec}.1}^2/d\ ;\ d_{02} \approx d + L_{\text{rec}.2}^2/d\ . \qquad (8)$$

In this case, the condition of space-time radio signal narrowband feature can be defined as follows:

$$L_{rec.i} << \sqrt{c\, d_i/\Delta f}\ ,\ i = 1,2\,, \qquad (9)$$

where $c = 3 \cdot 10^8$ m/s is the velocity of EMW propagation.

Consider the example when DRRS radio signal bandwidth $\Delta f = 40$ MHz and distances between central antennas of transmitting and receiving arrays are $d_1 = 5$ km, $d_2 = 10$ km, respectively. As a result, we find the limits of maximal base sizes that satisfy the condition (9): $L_{rec.i}^{(1)} << 194$ m, $L_{rec.i}^{(2)} << 274$ m, $i = 1,2$.

The expressions (6) describe conditions of space-time radio signal narrowband feature at receiving side of sparse antenna array when EMW are radiated by antennas $A_{1.tr}$ and $A_{2.tr}$. Considering the case when only antenna $A_{1.tr}$ radiates the electromagnetic wave, we can write

$$d_{12} \approx d_{10} + L_{rec.2} \sin\theta_1 + L_{rec.2}^2 \cos^2\theta_1/2d_{10}\ ; \qquad (10)$$

$$d_{11} \approx d_{10} - L_{rec.1} \sin\theta_1 + L_{rec.1}^2 \cos^2\theta_1/2d_{10}\ ; \qquad (11)$$

$$d_{10} = \sqrt{L_{tr.1}^2 + d^2}\ ;\ \theta_1 = \arctan(L_{tr.1}/d)\,. \qquad (12)$$

Substituting (10), (11) and (12) into (6), we obtain

$$(L_{rec.2}^2 - L_{rec.1}^2)\cos^2\theta_1/2d_{10} +$$
$$+ (L_{rec.2} + L_{rec.1})\sin\theta_1 - c/\Delta f << 0\,.$$

From the latter expression in the particular case when $L_{rec.2} = L_{rec.1}$ considered below, the condition of space-time radio signal narrowband feature can be represented as

$$L_{rec.1} = L_{rec.2} << c/(2\Delta f \sin\theta_1) . \quad (13)$$

According to (13) if $d_1 = 5$ km, $d_2 = 10$ km, $L_{tr.1} = 5$ m, $\Delta f = 40$ MHz, we get:

$$L_{rec.1}^{(1)} << 7500 \text{ m}; \; L_{rec.1}^{(2)} << 15{,}000 \text{ m}.$$

In general case when resolving the above considered inequality under condition $L_{rec.2} = kL_{rec.1}$, where $k > 1$, we obtain:

$$L_{rec.1} << \{-2d_{10}(k+1)\sin\theta_1 + +[4d_{10}^2(k+1)^2\sin^2\theta_1 + 8d_{10}c(k^2 - -1)\cos^2\theta_1 / \Delta f]^{1/2}\} / [2(k^2-1)\cos^2\theta_1] \quad (14)$$

Calculations show that in the case when $k \approx 1$, the results obtained by using the expression (14) coincide with those received by means of (13). Therefore, based on (9) and (13), the condition of space-time radio signal narrowband feature can be written as

$$L_{rec.i} = \min[c/(2\Delta f \sin\theta_1), \sqrt{c\,d_i/\Delta f}\,],\; i = 1,2 . \quad (15)$$

When one of the conditions (5) or (6) is fulfilled, one can consider that complex envelopes of desired signal (3) from different antennas of transmitting side at point *X* are almost the same:

$$\dot{S}_{tr}(t - d_{0x}/c) \approx \dot{S}_{tr}\left(t - d_{1x}/c\right) \approx \dot{S}_{tr}\left(t - d_{2x}/c\right), \quad (16)$$

what is equivalent to the condition $d_{0x} \approx d_{1x} \approx d_{2x} \approx d$.

When the condition (5) is fulfilled, the spatial and time structures of radio signal (3) can be analyzed independently from each other. In this case, the summarized radio signal can be presented as follows:

$$\dot{s}_0(t,x) = \alpha_0 \dot{S}_{tr}(t-\tau_0)\exp(j\omega_0 t) \times \times \sum_{i=0}^{2}[F_{i.tr}(\theta_{ix})\exp(-j\beta d_{ix})] = = \alpha_0 \dot{S}_{tr}(t-\tau_0)A(x)\exp[j\Phi(x)]\exp(j\omega_0 t) , \quad (17)$$

where $\exp(-j\beta d_{ix}) = \exp[-j(\omega_0 d_{ix})/c]$ denotes the multiplier that considers the phase shift of carrier along propagation path when signal comes into point *X*; $\tau_0 = d/c$ is the delay time of the radio signal on the distance between transmitting and receiving sparse antenna arrays.

According to (17), EMW amplitude and phase distributions on the continuous aperture of DRRS receiving side antenna can be described as follows:

$$A(x) = \left|\sum_{i=0}^{2} F_{i.tr}(\theta_{ix})\exp(-j\beta d_{ix})\right| = = \sqrt{[\sum_{i=0}^{2} F_{i.tr}(\theta_{ix})\cos(\beta d_{ix})]^2 + [\sum_{i=0}^{2} F_{i.tr}(\theta_{ix})\sin(\beta d_{ix})]^2} ; \quad (18)$$

$$\Phi(x) = \arg[\sum_{i=0}^{2} F_{i.tr}(\theta_{ix})\exp(-j\beta d_{ix})] , \quad (19)$$

where the function arg denotes the complex number argument varying from -180 to $+180$ degrees.

Pencil-beam pattern of transmitting parabolic reflector antenna described by formulas (18) and (19) from [7] can be written as follows:

$$F_0(\theta) = \left|J_1(2\varsigma)/\varsigma\right|\left(1+\cos\theta\right)/2 , \quad (20)$$

where $\varsigma = \pi a \sin\theta/\lambda$; $J_1(2\varsigma)$ is the Bessel function of the first order; a denotes the transmitting antenna half diameter. The pattern value defined by expression (20) depends on point *X* coordinate of receiving antenna continuous aperture because the angle θ is a function of x.

Using expressions (18), the calculations of amplitude and phase distributions on the continuous receiving side aperture have been carried out for the case when it is exited by the electromagnetic wave radiated by the transmitter T_1. The following initial data was used for the calculation: the operation frequency $f_0 = 15$ GHz, receiving aperture size $2L_{rec.1} = 24$ m, transmitting antenna diameter $2a = D_{tr} = 1$ m. Graphic charts of amplitude and phase distributions when $d = 5$ km are presented in Fig. 2 and Fig. 3 for three values of distance between radiating antennas: $L_{tr.1} = L_{tr.2} = 5$ m (solid curve), 10 m (dashed curve), 15 m (dot-dashed line). Corresponding to these data, limits of far-field regions defined in accordance with (1) are equal $D_{FF} = 12.1$ km; 44.1 km; 96.1 km, respectively.

Carrying out the analogy with (18) and (19) we can obtain the EMW amplitude and phase distributions on continuous receiving side aperture created by central transmitting antenna $A_{0.tr}$ shown in Fig. 1. As a result, we get:

$$A_{00}(x) = \left|F_{0.tr}(\theta_{0x})\exp(-j\beta d_{0x})\right| = = \sqrt{[F_{0.tr}(\theta_{0x})\cos(\beta d_{0x})]^2 + [F_{0.tr}(\theta_{0x})\sin(\beta d_{0x})]^2} ; \quad (21)$$

$$\Phi_{00}(x) = \arg[F_{0.tr}(\theta_{0x})\exp(-j\beta d_{0x})] . \quad (22)$$

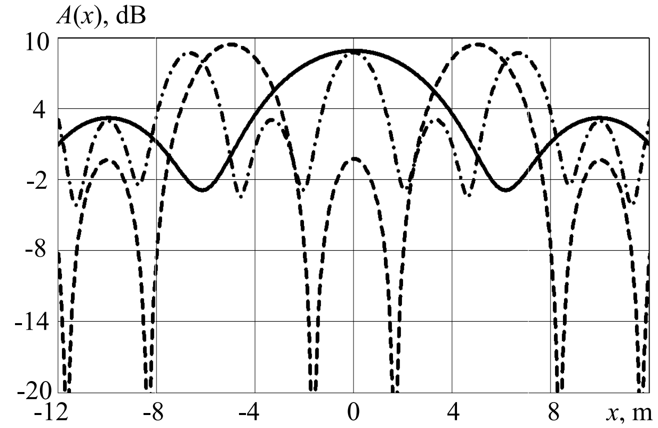

Fig. 2. Signal amplitude distribution of transmitter T_1 on continuous aperture of receiving side array when $d = 5$ km.

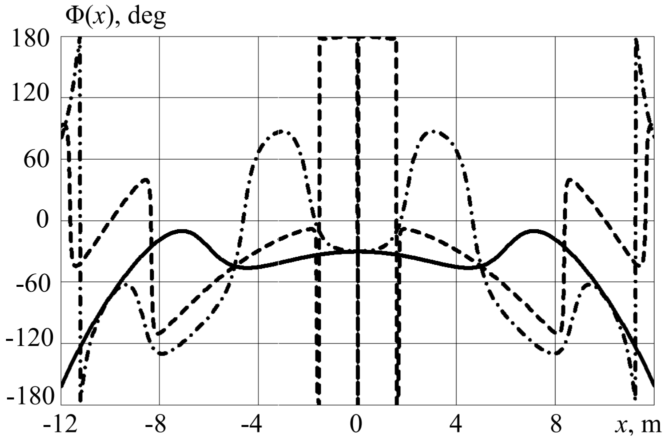

Fig. 3. Signal phase distribution of transmitter T_1 on continuous aperture of receiving side array when $d = 5$ km.

Graphic charts of EMW amplitude and phase distributions on the continuous receiving side aperture calculated in accordance with (21) and (22) for the case when the electromagnetic wave from transmitter T_2 is radiated from central element of transmitting antenna array are shown in Fig. 4 and Fig. 5 at the distances $d = 5$ km (solid curve) and $d = 10$ km (dashed curve).

Comparative analysis of results presented in Fig. 2 — Fig. 5 shows that EMW amplitude and phase distributions on the continuous receiving side aperture created by cophased coherent signals radiated by transmitting directional antennas of sparse antenna arrays at the distances $d = 5$ km and $d = 10$ km are not compliant with linear changing laws. Thus, the presented results evidently specify the availability of physical effect of EMW phase front curvature in the position of receiving side aperture placement. However, amplitude and phase oscillations decrease with growth of distance *d*. In this case, amplitude and phase distributions become more linear and the phase front straightens approaching to the plane one.

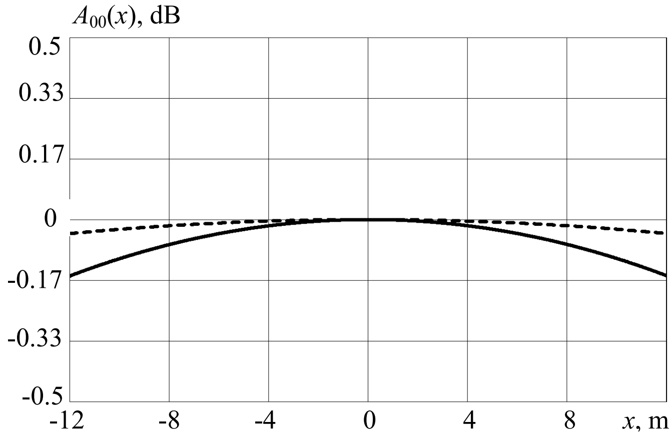

Fig. 4. Signal amplitude distribution of transmitter T_2 on continuous aperture of receiving side array.

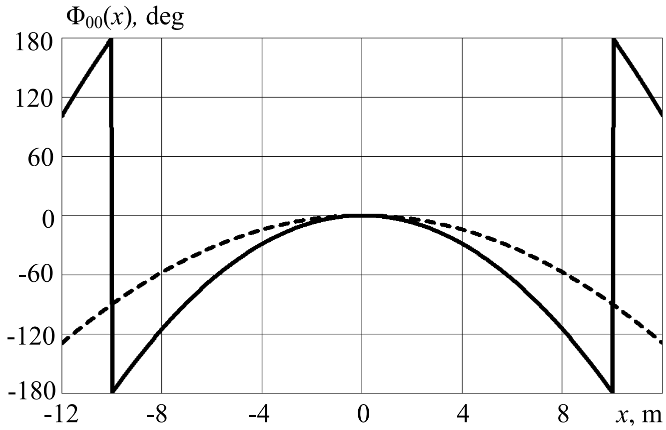

Fig. 5. Signal phase distribution of transmitter T_2 on continuous aperture of receiving side array.

Analysis of amplitude and phase distributions shown in Fig. 4 and Fig. 5 proves that even in the case of single transmitting antenna utilization, EMW phase front from transmitter T_2 on the aperture of receiving side array has the certain curvature. According to the condition (1), this transmitting antenna must be located inside the Fresnel zone of receiving antenna.

Efficiency estimation of optimal spatial signal processing in receiving sparse antenna array

Let us analyze an efficiency of spatial signal processing from two transmitters operating simultaneously in the same frequency band and with the same polarization but with different EMW phase front curvatures. The purpose of analysis is to define quantitative parameters allowing possibility of the radio signals separation from two transmitters at the receiving side of sparse antenna array.

In the 1st block of spatial processing (BSP) of receiving sparse antenna array, the signal of transmitter T_1 is considered as desired signal whereas the signal of transmitter T_2 is considered as an interference. In the 2nd block of spatial processing of receiving sparse antenna array, vice versa, the signal of transmitter T_2 is considered as desired signal whereas the signal of transmitter T_1 is considered as the interference. Taking into account that BSP principles are supposed to be equivalent, it is enough to consider functioning of only one BSP. Let us presume that bases of receiving sparse antenna array are the same and can be different in size: $L_{rec.1} = L_{rec.2} = x$.

In accordance with [8], all known optimal criteria of spatial signal processing are reduced to Wiener-Hopf equation

$$\mathbf{w}_{opt} = \mu \mathbf{R}_{NN}^{-1} \mathbf{S}_{\alpha}, \tag{23}$$

where μ is a constant defined by criterion of optimality; $\mathbf{R}_{NN}$ denotes the correlation matrix of receiver thermal noises and external interferences; $\mathbf{S}_{\alpha}$ is the column vector describing the amplitude and phase distributions of desired signal on the aperture of receiving antenna array; $\mathbf{w}_{opt}$ denotes the column vector of weighting coefficients showing how the amplitude and phase of summarized radio signal in each receiving channel should be changed to distinguish expected desired signal and suppress interference. According to [8], we can write

$$\dot{s}_{out}(t,x) = \mathbf{w}_{opt}^{H} \mathbf{s}_{in}(t,x), \tag{24}$$

where $\mathbf{s}_{in}(t,x)$ is the column vector of input desired space-time signal in channels of receiving antenna array that can be expressed as follows:

$$\mathbf{s}_{in}(t,x) = \mathbf{S}_{\alpha}(x)\dot{s}(t), \tag{25}$$

$\dot{s}(t) = \tilde{\alpha}_0 \dot{S}_{tr}(t - \tau_0)\exp(j\omega_0 t)$ is the time structure of desired signal; $\tilde{\alpha}_0 = \alpha_0 10^{-0.05 G_{rec}}$; G_{rec} denotes the single antenna gain of sparse antenna array, dB; $\mathbf{S}_{\alpha}^{T}(x) = \{\tilde{A}(-x)\exp[j\tilde{\Phi}(-x)], \tilde{A}(0)\exp[j\tilde{\Phi}(0)], \tilde{A}(x)\exp[j \times \tilde{\Phi}(x)]\}$ is the spatial structure of desired signal; $\tilde{A}(x)$ and $\tilde{\Phi}(x)$ are amplitude and phase distributions that are similar to (18), (19) and can be defined taking into account the influence of beam patterns of receiving antennas.

To simplify the analysis we can consider that $F_{i.tr}(\theta) = F_0(\theta)$, $i = \overline{0,2}$. As a result, we obtain

$$\tilde{A}(x) = \left| \sum_{i=0}^{2} F_0^2(\theta_{ix}) \exp(-j\beta d_{ix}) \right|;$$

$$\tilde{\Phi}(x) = \arg[\sum_{i=0}^{2} F_0^2(\theta_{ix}) \exp(-j\beta d_{ix})]. \tag{26}$$

According to [5, 8], we can define the correlation matrix for transmitter T_2 external interference and receiver noises at receiving side under condition that they are uncorrelated with each other:

$$\mathbf{R}_{NN} = \mathbf{R}_I + \mathbf{R}_0, \tag{27}$$

where $\mathbf{R}_I = \overline{\mathbf{n}_{in}(t,x)\mathbf{n}_{in}^{H}(t,x)}$ is the correlation matrix of the transmitter T_2 interference in channels of receiving antenna; $\mathbf{R}_0$ denotes the correlation matrix of receiver noises; $\mathbf{n}_{in}(t,x)$ is column vector of interference; the signs "—", "H" denote the statistical averaging in time and Hermitian conjugation, respectively. By the analogy with (25), we can consider that

$$\mathbf{n}_{in}(t,x) = \mathbf{N}_{\nu}(x)\dot{n}(t), \tag{28}$$

where $\dot{n}(t) = \tilde{\alpha}_0 \dot{N}_{tr}(t - \tau_0)\exp(j\omega_0 t)$ is the interference time structure; $\dot{N}_{tr}(t)$ denotes the interference complex envelope; $\mathbf{N}_{\nu}(x)$ is the interference spatial structure described as

$$\mathbf{N}_{\nu}^{T}(x) = \{\tilde{A}_{00}(-x)\exp[j\tilde{\Phi}_{00}(-x)], \tilde{A}_{00}(0) \times$$
$$\times \exp[j\tilde{\Phi}_{00}(0)], \tilde{A}_{00}(x)\exp[j\tilde{\Phi}_{00}(x)]\}, \tag{29}$$

$A_{00}(x) = \left| F_0^2(\theta_{0x})\exp(-j\beta d_{0x}) \right|$ denotes the EMW amplitude distribution (from transmitter T_2) at receiving side aperture taking into account the beam pattern of antenna elements of receiving sparse antenna array; $\Phi_{00}(x) = \arg[F_0^2(\theta_{0x})\exp(-j\beta d_{0x})]$ is the EMW phase distribution at receiving side aperture.

Considering the spatial structures of desired $\mathbf{S}_{\alpha}(x)$ and interfering $\mathbf{N}_{\nu}^{T}(x)$ signals as nonrandom time quantities, we can define that

$$\mathbf{R}_I = \mathbf{N}_{\nu}(x)\mathbf{N}_{\nu}^{H}(x)P_I, \quad 30)$$

where P_I is the average power of interfering signal.

When the receiver thermal noise is quasi-white Gaussian noise, the correlation matrix of receiver thermal noise can be defined as follows:

$$\mathbf{R}_0 = \overline{\mathbf{n}_0(t,x)\mathbf{n}_0^{H}(t,x)} = \mathbf{I}\sigma_0^2, \tag{31}$$

where $\mathbf{n}_0^{T}(t,x) = [\dot{N}_{01}(t), \dot{N}_{00}(t), \dot{N}_{02}(t)]$ is the column vector of the receiver noises in channels of receiving sparse antenna array; $\dot{N}_{0i}(t)$ denotes the complex envelope of quasi-white Gaussian noise in i th channel of receiving sparse antenna array, $i = \overline{0,2}$; $\mathbf{I}$ designates the unitary matrix; σ_0^2 is the average power of receiver noises of receiving sparse antenna array defining as follows

$$\sigma_0^2 = kT_N \Delta f, \tag{32}$$

where $k = 1.38 \cdot 10^{-23}$ W/Hz·K; T_N is the noise temperature of receiving side aperture.

Taking into account expressions (27)—(32), the column vector of weighting coefficients of spatial processing can be defined as follows

$$\mathbf{w}_{opt} = \mu / \sigma_0^2 \{\mathbf{I} - [h\mathbf{N}_\nu(x)\mathbf{N}_\nu^H(x)] / (1 + hM)\}\mathbf{S}_\alpha(x), \quad (33)$$

where $h = P_I / \sigma_0^2$ is the ratio of transmitter T_2 power (interference power) to receiver thermal noise power in single channel of receiving sparse antenna array.

If the external interference is absent, the expression (33) can be reformulated in such a way

$$\mathbf{w}_{0opt} = \mu / \sigma_0^2 \mathbf{S}_\alpha(x). \quad (34)$$

The coefficient of desired signal (from transmitter T_1) attenuation caused by spatial signal processing in the 1st block of spatial processing to distinguish the signal and to suppress interference (from transmitter T_2) can be defined as follows

$$F_{att} = 20\log[\dot{s}_{out.0}(t,x) / \dot{s}_{out}(t,x)] =$$
$$= -20\log[1 - \rho_{\alpha\nu}^2(x)], \quad (35)$$

where $\dot{s}_{out.0}(t,x) = \mathbf{w}_{0opt}^H \mathbf{s}_{in}(t,x)$ is the desired signal after its spatial processing against a background of receiver thermal noise in receiving sparse antenna array; $\rho_{\alpha\nu}(x) = \left|\mathbf{S}_\alpha^H(x)\mathbf{N}_\nu(x)\right| / M$ denotes the discrepancy function of nonrandom structures of desired signal and interference that describes differences in forms of their phase fronts in arbitrary point X of receiving side antenna array.

Figures 6 and 7 present graphic charts of attenuation coefficient calculated according to (35) versus the distance d between DRRS transmitting and receiving parts for different sizes of receiving antenna base: $x = 5$ m (solid curve); $x = 10$ m (dashed-line curve); $x = 15$ m (dot-dashed curve). The analysis of graphic charts presented in Fig. 6 and Fig. 7 shows that the growth of distance d between DRRS transmitting and receiving arrays under their fixed base sizes courses increasing the desired signal attenuation because phase fronts become more plane.

Figures 8 and 9 present graphic charts of attenuation coefficient calculated according to (35) versus the base size x of equidistant receiving sparse antenna array for different distances d: $d = 5$ km (solid curve); $d = 10$ km (dashed-line curve); $d = 15$ km (dot-dashed curve).

According to (35), the suppression coefficient of interference in the 1st BSP after optimal spatial processing can be derived as

$$K_{sup} = 20\log[\dot{n}_{out.0}(t,x) / \dot{n}_{out}(t,x)] =$$
$$= 20\log(1 + hM), \quad (36)$$

where $\dot{n}_{out.0}(t,x) = \mathbf{w}_{0opt}^H \mathbf{n}_{in}(t,x)$ denotes interfering signal at the output of the 1st BSP after spatial processing against receiver noise defined according to (34); $\dot{n}_{out}(t,x) = \mathbf{w}_{opt}^H \mathbf{n}_{in}(t,x)$ is interfering signal at the output of the 1st BSP after spatial processing against receiver noise determined according to (33).

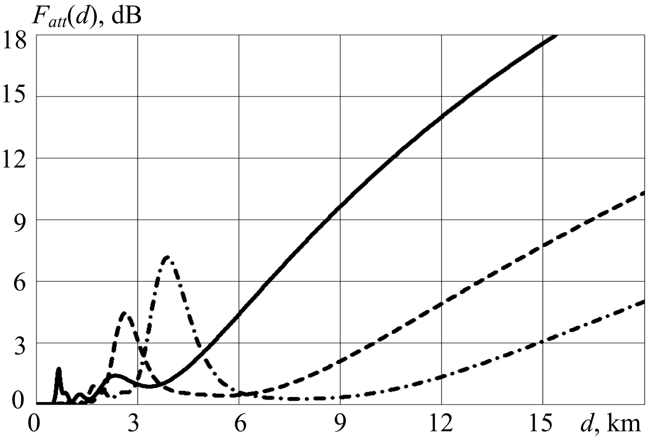

Fig. 6. Attenuation coefficient of desired signal versus the distance d when $L_{tr} = 5$ m.

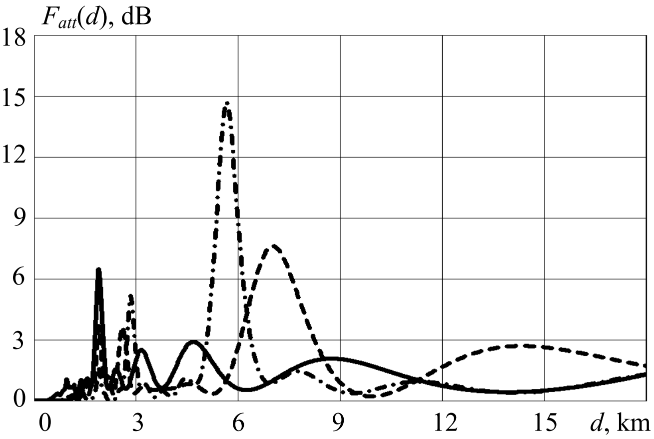

Fig. 7. Attenuation coefficient of desired signal versus the distance d when $L_{tr} = 15$ m.

The expression (36) shows that the suppression coefficient for interfering signal when optimal spatial processing is used does not depend on the form of EMW phase front.

The suppression coefficient is defined by the number of antenna elements M and also determined by power exceeding the receiver noise level. When $M = 3$ and $h = 1{,}000$ (30 dB); 4,000 (36 dB); 10,000 (40 dB) $K_{sup} = 69.5$; 81.5; 89.5 dB, respectively. Graphic charts shown in Fig. 8, Fig. 9 prove that attenuation coefficient decreases with increasing the base size of sparse antenna array.

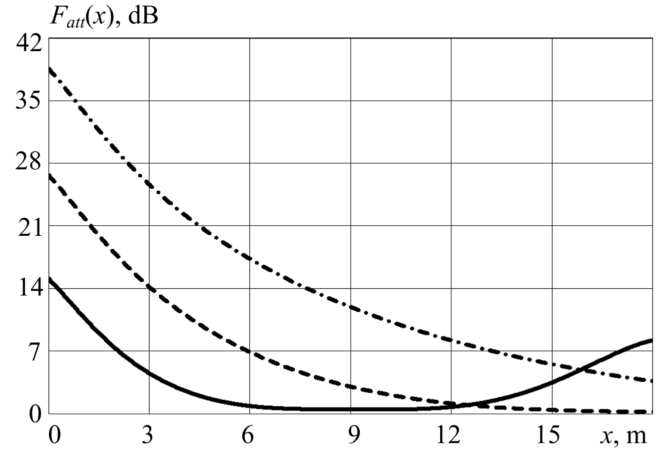

Fig. 8. Attenuation coefficient of desired signal versus the base size x of receiving antenna array at $L_{tr} = 5$ m.

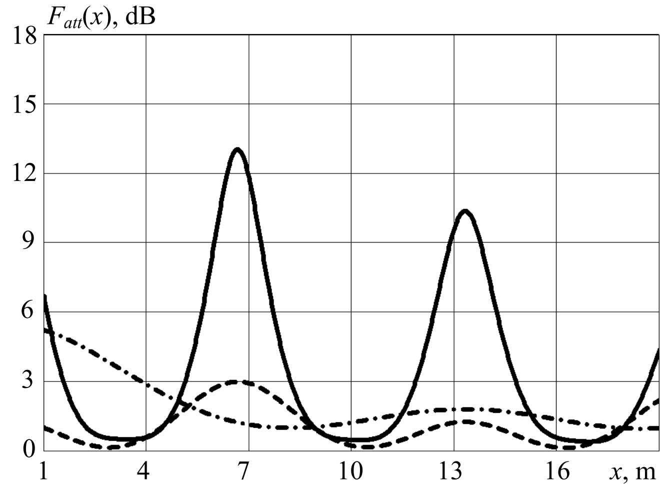

Fig. 9. Attenuation coefficient of desired signal versus the base size x of receiving antenna array at $L_{tr} = 15$ m.

The ratio of transmitter T_1 signal power to total interference power from transmitter T_2 and receiver noise $C/(I+N)$ at the output of receiving sparse antenna array after optimal spatial processing is given as:

$$Q = P_{s.out} / (P_{I.out} + P_{0.out}); \quad (37)$$

$$P_{s.out} = \mathbf{w}_{opt}^H \overline{\mathbf{s}_{in}(t,x)\mathbf{s}_{in}^H(t,x)} \mathbf{w}_{opt};$$

$$P_{I.out} = \mathbf{w}_{opt}^H \overline{\mathbf{n}_{in}(t,x)\mathbf{n}_{in}^H(t,x)} \mathbf{w}_{opt};$$

$$P_{0.out} = \mathbf{w}_{opt}^H \overline{\mathbf{n}_0(t,x)\mathbf{n}_0^H(t,x)} \mathbf{w}_{opt}.$$

Here $P_{s.out}$, $P_{I.out}$, $P_{0.out}$ denote the desired signal power, the interference power and the receiver thermal noise power, respectively, after spatial processing.

As a result, we get

$$Q = Q_{SNR} \mathbf{w}_{opt}^H \mathbf{S}_\alpha(x) \mathbf{S}_\alpha^H(x) \mathbf{w}_{opt} / [h \times \times \mathbf{w}_{opt}^H \mathbf{N}_\nu(x) \mathbf{N}_\nu^H(x) \mathbf{w}_{opt} + \mathbf{w}_{opt}^H \mathbf{w}_{opt}], \quad (38)$$

where $Q_{SNR} \geq Q_{SNR\min}$ denotes the carrier-to-interference ratio C/I at the receiver input without spatial processing; $Q_{SNR\min}$ is the minimal C/I ratio ensuring required probability at the output of receiver demodulator.

Graphic charts shown in Figures 10, 11 represent dependences of $C/(I+N)$ ratio calculated according to (38) with $Q_{SNR} = 40$ dB as the functions of distance d between DRRS transmitting and receiving antennas for different sizes of receiving antenna array: $x = 5$ m (solid curves); $x = 10$ m (dashed-line curves); $x = 15$ m (dot-dashed curves). These charts show that maximal $C/(I+N)$ ratio is achieved at the distance d between DRRS transmitting and receiving side arrays approximately equal to the initial one without spatial processing. For example, considering the cases $x = 5$ m, $d = 3.5$ km and $x = 15$ m, $d = 8.5$ km, when minimal required value of $C/(I+N)$ ratio is 33 dB, for QAM-64 we obtain $Q_{\max} = 30$; 33.5 dB, respectively.

Graphic charts shown in Figures 12, 13 represent the $C/(I+N)$ ratio according to (38) versus the sizes of receiving antenna array for different distances d between DRRS transmitting and receiving antennas: $d = 5$ km (solid curve); $d = 10$ km (dashed-line curve); $d = 20$ km.

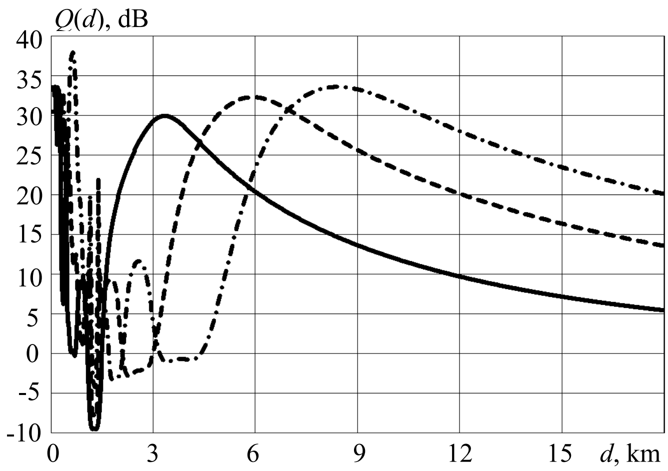

Fig.10. Graphic charts of $C/(I+N)$ ratio versus the distance d at $L_{tr} = 5$ m.

Figures 12, 13 show that the growth of base size of transmitting antenna array leads to increasing the maximal $C/(I+N)$ ratio that exceeds $Q_{SNR\min} = 33$ dB after spatial processing. This result is achieved due to increasing the difference in curvatures of EMW phase fronts at the aperture of receiving sparse antenna array arriving from different transmitters.

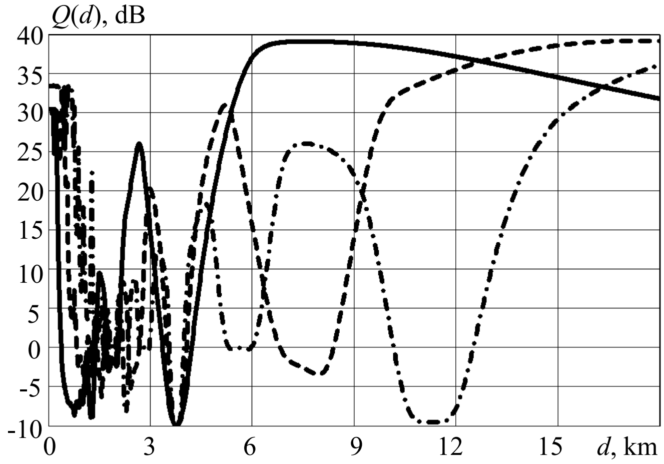

Fig. 11. Graphic charts of $C/(I+N)$ ratio versus the distance d at $L_{tr} = 15$ m.

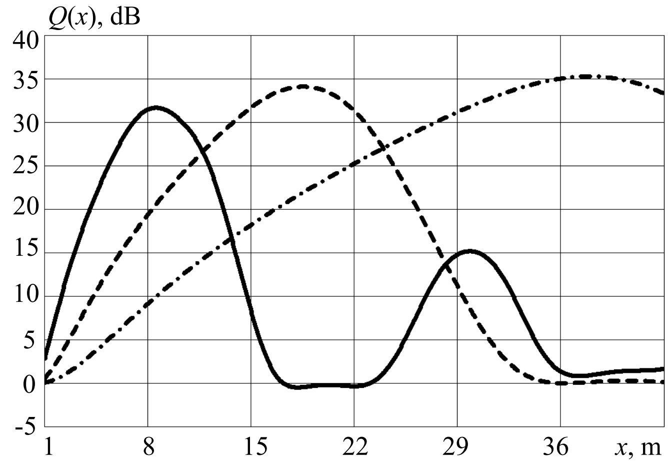

Fig. 12. Graphic charts of $C/(I+N)$ ratio versus the size of base x of receiving sparse antenna array at $L_{tr} = 5$ m.

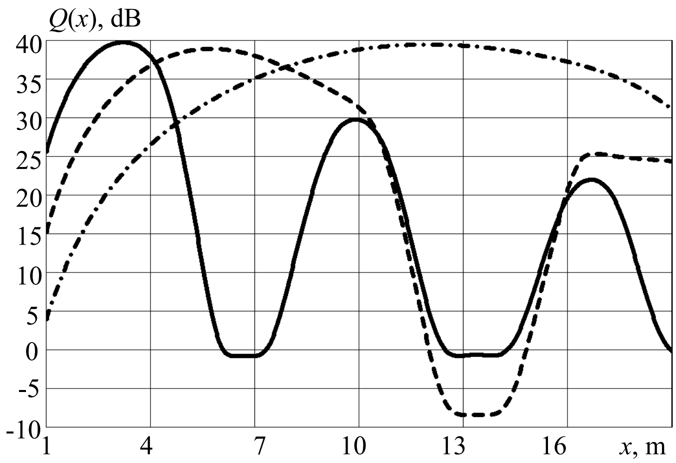

Fig. 13. Graphic charts of $C/(I+N)$ ratio versus the size of base x of receiving sparse antenna array at $L_{tr} = 15$ m.

Conclusion

Results of mathematical modeling demonstrate the possibility of application of physical effect of EMW phase front curvature at aperture of receiving sparse antenna array to create the radio relay links with frequency reuse. The efficient algorithm of optimal spatial signal processing in receiving sparse antenna array has been proposed to separate two radio signals from each other by using the form of EMW phase front. The simultaneous transmission of desired and undesired signals at the same frequency and polarization has been investigated. It is shown that maximal efficiency of spatial processing in receiving sparse antenna array when the distance between transmitter and receiver is fixed is achieved if sizes of receiving antenna array bases are selected in such a way that $C/(I+N)$ ratio exceeds the required $(C/I)_{\min}$ ratio for chosen modulation form.

The proposed method of spatial processing can be used to construct digital radio relay systems providing the simultaneous transmission of information from two different sources in the same frequency band.

References

1. Ilchenko M. E., Narytnik T. N., Ilushko V. M. Combined modulation method application in microwave links // Radioelectronics and Computer Systems. — 2009. — N. 2 (36). — P. 71—77 [in Russian].

2. Nikitchenko V. V., Gladkih S. N., Vihlyantsev P. S. Analysis of discrimination possibility of radiation sources with usage phase front curvature // Radioelectronics and Communications Systems. — 1988. — Vol. 31, N. 7. — P. 58—60.

3. Avdeyenko G. L., Fedorov V. I., Yakornov Ye. A. Determination of the radiation source location based on the electromagnetic wave front curvature // Radioelectronics and Communications Systems. — 2008. — Vol. 51, N. 3. — P. 115—121.

4. Avdeyenko G. L., Lipchevskaya I. L., Yakornov Ye. A. Phase systems of determining coordinates of radiation source with harmonic signal in Fresnel zone // Radioelectronics and Communications Systems. — 2012. — Vol. 55, N. 2. — P. 65—74.

5. Space-time signal processing / I. Y. Kremer, A. I. Kremer, V. M. Petrov, et al. — Moscow: Radio i Svyaz, 1984. — 224 p. [in Russian].

6. Slyusar V. I. Correction of characteristics of receiving channels in a digital antenna array by a test source in the near zone // Radioelectronics and Communications Systems. — 2003. — Vol. 46, N. 1. — P. 30—35.

7. Aizenberg G. Z. Antennas UHF. — Moscow: Svyaz, 1977. — 288 p. [in Russian].

8. Monzingo R. A., Haupt R. L., Miller T. W. Introduction to adaptive arrays. — SciTech Publishing, 2011. — 560 p.

Received in final form July 19, 2012